

# Synthesis, characterization and performance of vanadium hexacyanoferrate as electrocatalyst of H<sub>2</sub>O<sub>2</sub>

Constantinos G. Tsiafoulis<sup>a</sup>, Pantelis N. Trikalitis<sup>b</sup>, Mamas I. Prodromidis<sup>a,\*</sup>

<sup>a</sup> Department of Chemistry, Laboratory of Analytical Chemistry, University of Ioannina, Dourouti, 45 110, Ioannina, Greece

<sup>b</sup> Department of Chemistry, University of Crete, 71 409, Heraklion Crete, Greece

Received 26 September 2005; received in revised form 30 September 2005; accepted 3 October 2005

Available online 4 November 2005

## Abstract

The present work reports for the first time on the synthesis, characterization and performance of vanadium hexacyanoferrate (VHCF) as electrocatalyst of hydrogen peroxide. VHCF was synthesized by mixing V<sub>2</sub>O<sub>5</sub> · nH<sub>2</sub>O xerogel with ascorbic acid and K<sub>4</sub>[Fe(CN)<sub>6</sub>] in double distilled water. X-ray powder diffraction, energy dispersive spectroscopy, scanning electron microscopy, and IR-spectroscopy data suggest the formation of nanocrystalline (mean crystal size ~11 nm) compound with a tentative molecular formula K<sub>2</sub>(VO)<sub>3</sub>[Fe(CN)<sub>6</sub>]<sub>2</sub>. Composite films of VHCF with poly(vinyl alcohol) were developed over a glassy carbon electrode, and then covered with different (neutral, positively or negatively charged) membranes. The effect of each membrane on the working stability of the resultant sensors was evaluated. Cyclic voltammetry experiments showed that composite films exhibit a pair of reversible redox peaks, and a remarkable low potential electrocatalysis on both the reduction and oxidation of hydrogen peroxide. A linear calibration curve over the concentration range 0.01–3.0 mM H<sub>2</sub>O<sub>2</sub> was constructed. Limit of detection (*S/N* = 3) of 4 μM H<sub>2</sub>O<sub>2</sub> was calculated. The proposed transducer is quite selective to hydrogen peroxide. No response was observed in the presence of 10 mM ascorbic acid.

© 2005 Elsevier B.V. All rights reserved.

**Keywords:** Vanadium hexacyanoferrate; Prussian blue analogue; Hydrogen peroxide chemical sensor

## 1. Introduction

The detection of H<sub>2</sub>O<sub>2</sub> is important in environmental, food, and industrial analysis; it is used to pollution control, to bleach textiles and paper products, and to manufacture or process foods, minerals, petrochemicals, and consumer products. It is also fundamental for the development of biosensors based on oxidase enzymes [1].

Electrochemical detection of hydrogen peroxide by its oxidation at a variety of electrode materials requires a high overpotential (>+0.65 V versus common reference electrodes). This electrode potential is high enough to produce a considerable loss of selectivity in the presence of interfer-

ing species as well as to cause a gradual decrease of the sensitivity of the electrode due to fouling phenomena [2].

The use of mediators has been proved as an effective approach to restrict or eliminate these problems; however, they may facilitate charge transfer between possible interferants and the electrode, or in the case of immobilized mediators, they may be washed out to the bulk electrolyte, producing thus a progressively diminishing response to the analyte [3].

Another strategy to lower the applied potential for the detection of hydrogen peroxide is the use of peroxidases [4,5] as bioelectrocatalysts for the electrochemical reduction of hydrogen peroxide. In this case, the electron transfer between the enzyme and the electrode surface can be obtained either directly or through a mediator.

In this perspective, various redox compounds [1–3] and in particular Prussian blue (ferric hexacyanoferrate, PB) have found a large use. Prussian blue, Fe<sub>4</sub><sup>III</sup>[Fe<sup>II</sup>(CN)<sub>6</sub>]<sub>3</sub> ·

\* Corresponding author. Tel.: +30 26510 98301; fax: +30 26510 98796.  
E-mail addresses: [ptrikal@chemistry.uoi.gr](mailto:ptrikal@chemistry.uoi.gr) (P.N. Trikalitis), [mprodrom@cc.uoi.gr](mailto:mprodrom@cc.uoi.gr) (M.I. Prodromidis).

$n\text{H}_2\text{O}$ , the so-called “insoluble” form, and  $\text{KFe}^{\text{III}}\text{-Fe}^{\text{II}}(\text{CN})_6$ , the so-called “soluble” form (these terms refer to peptization rather than solubility), is a mixed valence compound [6]. The reduced form of PB had a catalytic effect for the reduction of molecular oxygen and hydrogen peroxide at low applied potentials of ca.  $-0.1$  to  $0.0$  mV versus Ag/AgCl [7,8]. The mechanism of catalysis of PB towards the reduction of  $\text{H}_2\text{O}_2$  is still not completely clear, probably due to the fact that there is still no complete agreement concerning its structure and its stoichiometric composition. The zeolitic nature of PB with a cubic unit cell of  $10.2$  Å and with channel diameters of about  $3.2$  Å allows the diffusion of low molecular weight molecules (such as  $\text{O}_2$  and  $\text{H}_2\text{O}_2$ ), whereas molecules with higher molecular weight such as ascorbic acid, uric acid and paracetamol (the commonest electroactive interferants) cannot diffuse into PB’s catalytic centre [7,9].

According to Itaya et al. [10], the structure and, in some extent, the catalytic properties of PB are depending on the materials and the procedure used for its formation. Moreover, the electrochemical activity of PB is supported in the presence of  $\text{K}^+$ ,  $\text{Rb}^+$ ,  $\text{Cs}^+$  and  $\text{NH}_4^+$  ions, in contrast to all group II cations ( $\text{Na}^+$ ,  $\text{Li}^+$ ,  $\text{H}^+$ ). In the presence of the latter, the activity of PB is blocked [11]. This is probably the origin of the most important disadvantages encountered in the use of PB in amperometric biosensors, i.e., poor working stability and sensitivity to pH-changes. The increase of solubility of PB at  $\text{pH} > 6$ , due to the formation of  $\text{Fe}(\text{OH})_3$ , restrains also its use in bioassays coupled with enzymes which have optimum pH at slight acidic to neutral region. A general overview on the electrochemistry and sensing aspects of Prussian blue-based hydrogen peroxide sensors is given in the comprehensive review of Ricci and Palleschi [12].

Similar to ferric hexacyanoferrate, transition metal hexacyanoferrate (MHCF), a class of polynuclear inorganic compounds, has also been proposed as electrocatalysts for hydrogen peroxide [13–27]. Among them, vanadium hexacyanoferrate films, structurally related to Prussian blue, have been electrodeposited from acidic solutions; however, their possible use as electrocatalysts of  $\text{H}_2\text{O}_2$  has not been explored [28–32].

We propose here for the first time the synthesis of vanadium hexacyanoferrate material by mixing  $\text{V}_2\text{O}_5 \cdot n\text{H}_2\text{O}$  xerogel with ascorbic acid and  $\text{K}_4[\text{Fe}(\text{CN})_6]$  in double distilled water. The electrochemical behaviour of VHCF/polyvinyl alcohol composite films was studied. Cycling voltammetry experiments support the efficiency of VHCF-based chemical sensor to provide a low potential detection of hydrogen peroxide at neutral pH. Analytical prospective of the proposed sensor is also demonstrated. Films were protected with neutral (polycarbonate), negatively (Nafion) and positively (polyethyleneimine) charged membranes, and the effect of each membrane on the working stability of the sensors was also investigated. The proposed sensor is also highly selective to the target analyte and works at sufficient low potentials minimizing thus foul-

ing effects on the electrode surface as well as the interference effect of various electroactive compounds. No interference signal was observed even in the presence of  $10$  mM ascorbic acid.

## 2. Experimental

### 2.1. Chemicals

Tris base and Tris–HCl salt were obtained from Sigma (USA). Potassium hexacyanoferrate(II) and Nafion (5% in aliphatic alcohol) were obtained from Sigma–Aldrich (UK). Polyethyleneimine (PEI) and photocrosslinkable polyvinyl alcohol with styrylpyridinium residues (PVA–SbQ) were purchased from Supelco (USA) and Toyo Gosei Kogyo (Japan), respectively. Isopore polycarbonate membranes (porosity  $0.1$  µm, thickness  $10$  µm) were purchased from Millipore (USA). Double distilled water (DDW) was used throughout. A stock solution of approximately  $0.2$  M  $\text{H}_2\text{O}_2$  was prepared by appropriate dilution of the concentrated solution (30%  $\text{H}_2\text{O}_2$ , Fluka) in DDW, stored at  $+4$  °C and was weekly standardized with the  $\text{KMnO}_4$  titrimetric method.

### 2.2. Apparatus

For the electrochemical experiments a computer-controlled potentiostat, Autolab12 by EcoChemie (The Netherlands), was used. Cyclic voltammetry was performed in a three-electrode voltammetry cell using a glassy carbon (GC) electrode ( $3$  mm diameter, BAS) as the working electrode, a Ag/AgCl/3 M KCl (BAS) reference electrode, and a Pt wire as auxiliary electrode. Before use, working electrodes were polished over a cotton cloth with fine aluminum oxide slurry, washed thoroughly with DDW and finally sonicated for  $3$  min in DDW and ethanol. Energy dispersive spectroscopy (EDS) analysis was performed using an ISIS-300 microanalysis system by Oxford Instruments (UK) in combination with a JEOL JSM-5600 scanning electron microscope (Japan). FTIR spectra were recorded using a Perkin–Elmer (USA) spectrometer. X-ray powder diffraction (Cu  $\text{K}\alpha$  radiation,  $\lambda = 1.5418$  Å) was performed with a Brüker D8 advance (Germany) in the range  $5^\circ < 2\theta < 50^\circ$  with a resolution of  $0.02^\circ$  ( $2\theta$ ).

### 2.3. Preparation of $\text{K}_2(\text{VO})_3[\text{Fe}(\text{CN})_6]_2$ powder (VHCF)

$\text{V}_2\text{O}_5 \cdot n\text{H}_2\text{O}$  xerogel was prepared according to the previous described procedure [33].  $1.206$  g ( $1.43$  mmol)  $\text{K}_4[\text{Fe}(\text{CN})_6]$  was dissolved in  $75$  mL DDW, followed by addition of  $0.5$  g ( $2.38$  mmol) of  $\text{V}_2\text{O}_5 \cdot n\text{H}_2\text{O}$  xerogel and  $1$  g of ascorbic acid. The mixture was incubated for  $48$  h at  $60$  °C. The product (a green powder) was isolated by filtration through a Gooch 3 crucible, washed thoroughly with DDW and acetone and allowed to air-dry overnight.

#### 2.4. Casting of PVA–SbQ/VHCF composite films

An amount of 1 g PVA–SbQ polymer was diluted with 2.0 mL of DDW (50% w/v), followed by addition of 10 mg VHCF. The mixture was sonicated for 5 min and then left to become homogenous under strong agitation overnight (the mixture is not perfectly homogenous).

#### 2.5. Electrode assembly

A portion of 3  $\mu\text{L}$  of PVA–SbQ/VHCF was pipetted onto the surface of the electrode and spin-coated at 1500 rpm for 2 min. The film was then left to air-dry overnight (thickness  $\approx 20 \mu\text{m}$ ). Before use, modified electrodes were exposed to UV irradiation (wavelength 365 nm) for 30 min. Finally, an aliquot of 3  $\mu\text{L}$  of an aqueous solution of 0.1% Nafion was applied over the films, and left to air-dry. Polycarbonate membranes (plain or modified by dropping 5  $\mu\text{L}$  of a 5% PEI in water) were placed with the aid of an O-ring.

#### 2.6. Determination of $\text{H}_2\text{O}_2$

**Steady-state amperometry:** (10.0 –  $x$ ) mL of 50 mM Tris buffer, pH 7, was introduced in the reaction cell and stirred at a moderate speed with a magnetic stirrer. When a stable current value was reached, appropriate volume [ $x$ ] mL of  $\text{H}_2\text{O}_2$  was added and current change at  $-0.15 \text{ V}$  versus Ag/AgCl/3 M KCl was recorded. The steady-state current response was taken as a measure of  $\text{H}_2\text{O}_2$  concentration.

### 3. Results and discussion

#### 3.1. Characterization of VHCF

The XRD pattern of the solid obtained by mixing  $\text{V}_2\text{O}_5 \cdot n\text{H}_2\text{O}$  xerogel fine powder with ascorbic acid and  $\text{K}_4[\text{Fe}(\text{CN})_6]$  in DDW is shown in Fig. 1. The pattern shows three broad Bragg peaks which can be indexed as the (200), (220) and (400) reflections of cubic lattice with unit cell size  $a = 10.1 \text{ \AA}$  and matches very well with that of crystalline  $\text{K}_2(\text{VO})_3[\text{Fe}(\text{CN})_6]_2$  reported in the literature [29,34]. This compound is a vanadium Prussian blue analogue that contains  $[\text{V}^{\text{IV}}\text{O}]^{2+}$  (vanadyl) and  $\text{Fe}^{\text{II}}$  ions in the structure [29,35]. The EDS analysis shows the presence of K, V and Fe in a ratio close to 2:3:2 as expected from the stoichiometric formula  $\text{K}_2(\text{VO})_3[\text{Fe}(\text{CN})_6]_2$ .

The presence of vanadyl ions and  $[\text{Fe}(\text{CN})_6]^{4-}$  complex ion is confirmed by infrared spectroscopy. Shown in Fig. 2 is the IR spectra of VHCF solid where the sharp peak at  $980 \text{ cm}^{-1}$  is characteristic of  $\text{V}=\text{O}$ . Moreover, the sharp peak at  $2095 \text{ cm}^{-1}$  is the characteristic stretching frequency of  $-\text{C}\equiv\text{N}$  ligand in  $[\text{Fe}(\text{CN})_6]^{4-}$  anion present in the VHCF solid, in full agreement with the literature data [34,36].

A representative SEM image is shown in Fig. 3, where an agglomeration of small particles is clearly visible

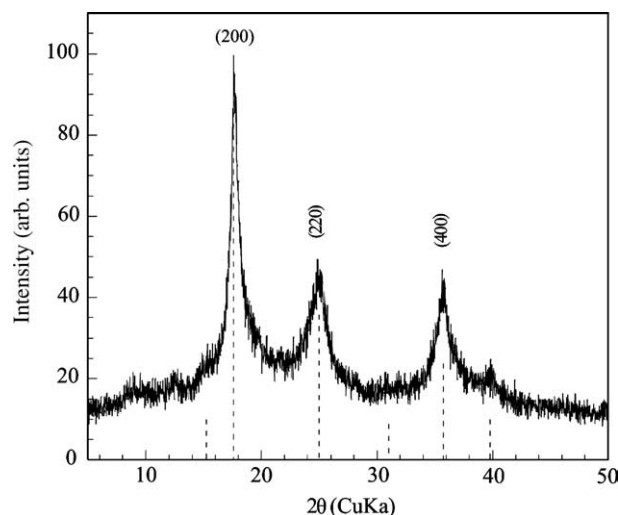


Fig. 1. XRD pattern of VHCF solid. The vertical dotted lines represent the data from JCPDS PDF# 42-1440 corresponding to  $\text{K}_2(\text{VO})_3[\text{Fe}(\text{CN})_6]_2$  material.

throughout the sample. These results are consistent with XRD data where the broad Bragg peaks observed indicate a small crystallite size. Based on Sherrer's equation using the full width at half-maximum intensity in X-ray diffraction reflection (200), the mean crystal size is estimated to be  $\sim 11 \text{ nm}$ .

The facile, one-pot synthesis of nanocrystalline VHCF electroactive material was accomplished via an in situ reduction of  $\text{V}_2\text{O}_5 \cdot n\text{H}_2\text{O}$  xerogel using ascorbic acid in the presence of  $\text{K}_4[\text{Fe}(\text{CN})_6]$ . Although this is almost a solid-to-solid transformation, the method is reproducible and yields pure phase in high yield. It is important to note that in the absence of ascorbic acid, a non-electroactive amorphous material was received.

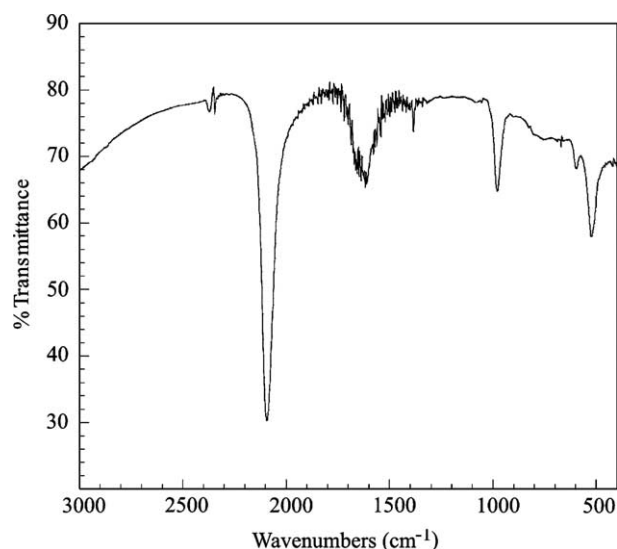


Fig. 2. Infrared spectrum of VHCF material.

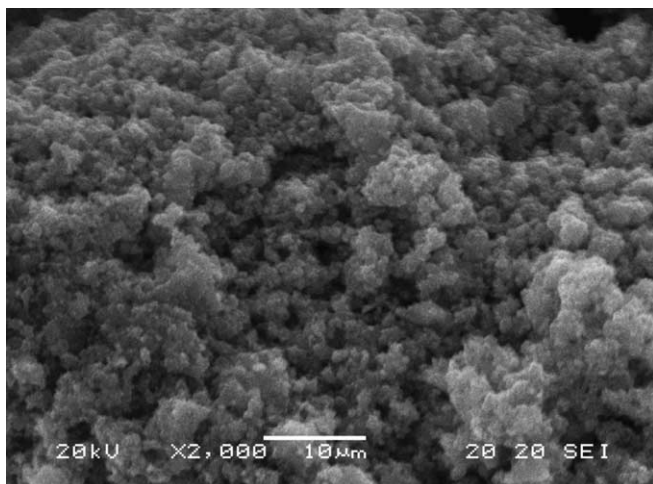


Fig. 3. Representative SEM image of VHCF material.

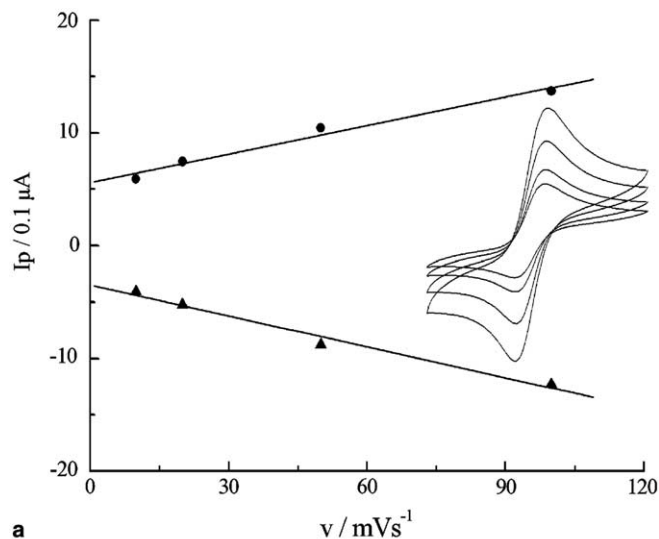
### 3.2. Electrochemistry of PVA–SbQ/VHCF films

Most of the electrochemical studies that have been performed up to now evaluate the voltammetric behaviour of VHCF in strong acidic media [28–32]. Under these conditions, cyclic voltammograms of VHCF exhibit two pairs of peaks [29,30,32], or three pairs of peaks [28,31] in the case of even stronger ( $>3.2$  M  $\text{H}_2\text{SO}_4$ ) acidic conditions. However, Carpenter et al. [29] failed to receive this extra peak even at concentrations higher than 3.2 M  $\text{H}_2\text{SO}_4$ . Results are also contradictory regarding the origin of the two pairs of peaks observed under the same experimental conditions. XPS data provide evidence that multiple ferrous sites are responsible for the CVgrams pattern of VHCF [29], while the involvement of both vanadium and iron redox centres has also been reported [29,30,32].

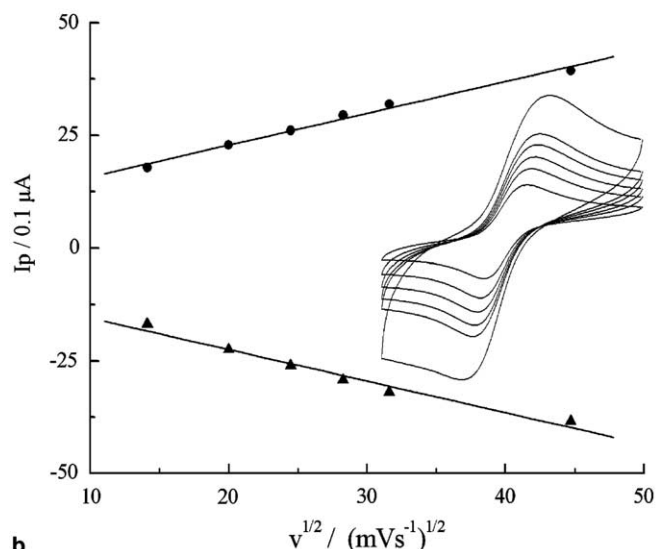
In the present study, the electrochemical behaviour of Nafion/VHCF/PVA–SbQ films was tested in a 50 mM Tris, pH 7, buffer solution, at various scan rates. CVgrams (Fig. 4a, b, Insets graphs) exhibit a well-defined pair of reversible peaks, probably attributable to a redox reaction of the electroactive iron sites ( $\text{Fe}^{\text{II}} \leftrightarrow \text{Fe}^{\text{III}}$ ).

Plots of the anodic and cathodic peak currents for the reduction and oxidation of the  $\text{Fe}^{\text{II}} \leftrightarrow \text{Fe}^{\text{III}}$  couple versus the potential scan rate,  $v$ , were linear from 0.01 to  $0.1 \text{ V s}^{-1}$  (Fig. 4a), suggesting facile charge transfer kinetics over this range of sweep rates. At faster scan rates however, from  $0.2$  to  $2 \text{ V s}^{-1}$  the relationship becomes linear only when current values plotted versus the square root of  $v$  (Fig. 4b) indicating mass transport limited within the composite film. This is specifically true in a regime of high surface coverage, as it happens in the case of VHCF material in the polymeric matrix, and high sweep rates. Under these high sweep rates, the diffusion step dominates the procedure. The diffusion mechanism is presumably attributable to electron transfer (hopping) among the mediator redox centres.

The separation between the anodic and cathodic peak potentials,  $\Delta E_p$ , values for scan rates  $0.01$ – $0.1 \text{ V s}^{-1}$  is



a



b

Fig. 4. Variation of  $I_p$  with (a) the scan rate and (b) the square root of scan rate for the PVA–SbQ/VHCF electrodes. Insets: Cyclic voltammograms represent the experimental data for scan rates: (a) 0.01, 0.02, 0.05,  $0.1 \text{ V s}^{-1}$  and (b) 0.2, 0.4, 0.6, 0.8, 1.0,  $2.0 \text{ V s}^{-1}$ . Buffer solution: 50 mM Tris, pH 7.

$70$ – $80 \text{ mV}$ , while for scan rates  $0.2$ – $2 \text{ V s}^{-1}$  the  $\Delta E_p$  varies between 110 and 214 mV. The ratios of anodic and cathodic peak current intensities,  $I_a/I_c$ , moderate from 1.28 to 1.04 (for scan rates  $0.01$ – $0.1 \text{ V s}^{-1}$ ) and from 0.95 to 0.84 (for scan rates  $0.2$ – $2.0 \text{ V s}^{-1}$ ). The observed non-ideal electrochemical behaviour of the films can be attributed to strong interactions between encapsulated molecules in the polymeric film as well as to surface structural heterogeneity of the latter [37].

The (apparent) electron transfer rate constants  $k^0$  were calculated from Tafel diagrams, using the theoretical value 0.5 for the charge transfer coefficient. Fig. 5 illustrates the procedure used for evaluating  $k^0$  from the anodic and cathodic partial reaction. Mean values of  $k^0 = 9.0 \pm 1 \text{ s}^{-1}$  were evaluated from all the extracted experimental data applying equation  $k^0 = 2.303anFv_0/RT$ .

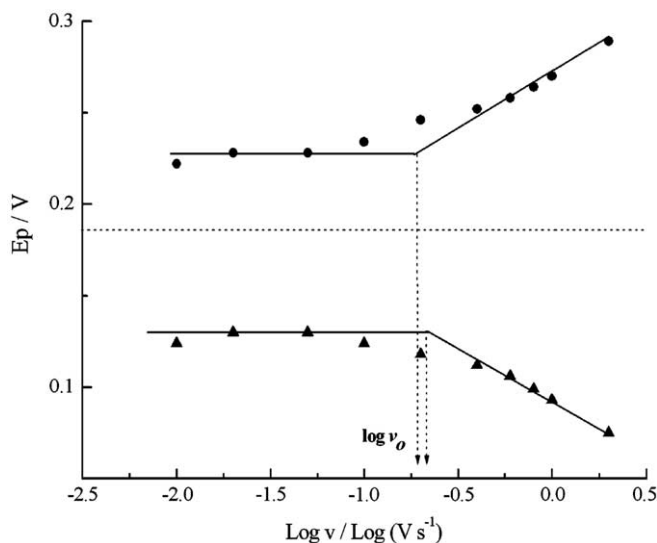


Fig. 5. Dependence of  $E_p$  on  $\log(v)$  for the PVA-SbQ/VHCF electrodes. Graphical calculation of the critical scan rate  $v_0$ . Buffer: 50 mM Tris, pH 7.

### 3.3. Stability studies

Similar to Prussian blue, metal cations have an important role to the electrochemical activity of VHCF films and consequently on the working stability of the resultant sensors. VHCF has a special character because both the metallic  $M^+$  ( $Li^+$ ,  $Na^+$ ,  $K^+$ ) and  $H^+$  cations participate in the redox process [30,38].

Trying to build up an electrode assembly that is potentially electrochemically inert on the composition of the working electrolyte and consequently on the composition of the matrix of real samples, we performed the following experiments and some preliminary results are discussed.

The stability of three different PVA-SbQ/VHCF electrodes, covered with neutral (polycarbonate), negatively charged (Nafion) and positively charged (PEI) membranes, respectively, was studied in a 50 mM phosphate, pH 7, buffer solution by performing cyclic voltammetry at the potential window +0.6 and -0.2 V at 0.2 V/s.

In the case of the neutral coating, sodium cations enter the redox film through a diffusion mechanism and a loss of about 20–25% of the original activity was observed after the completion of 1000 scans (Fig. 6a). In the case of the positively charged membrane, the diffusion of sodium cations into the redox film is restricted on the basis of a charge repulsive mechanism and after a conditioning period during the first 300 scans the redox response reaches a maximum value, which remains almost constant after 1000 scans (Fig. 6b). On the other hand, a considerable loss of the initial redox response was observed when redox films were covered with the negatively charged membrane. Sodium cations are strongly attracted by outermost sulfo groups and then pass from the Nafion membrane to the redox film blocking somehow the activity of the redox film (Fig. 6c). We assume that sodium cations replace protons in the VHCF structure, since the same electrode assembly (Nafion/PVA-SbQ/VHCF) exhibits an improved working stability by replacing phosphate buffer with Tris base/Tris-HCl buffer solution (Fig. 6d). The bulk tris(hydroxymethyl)aminomethane molecules cannot probably penetrate the VHCF lattice, thus allowing protons to charge compensate the redox reaction. In more basic pH values, however, the stability of the electrodes is considerably lower (Fig. 6e, f). The effect of sodium cations may differ at different concentrations of it, in accordance with previous studies regarding the effect of potassium cations on the redox activity of Nafion-protected Prussian blue films [39].

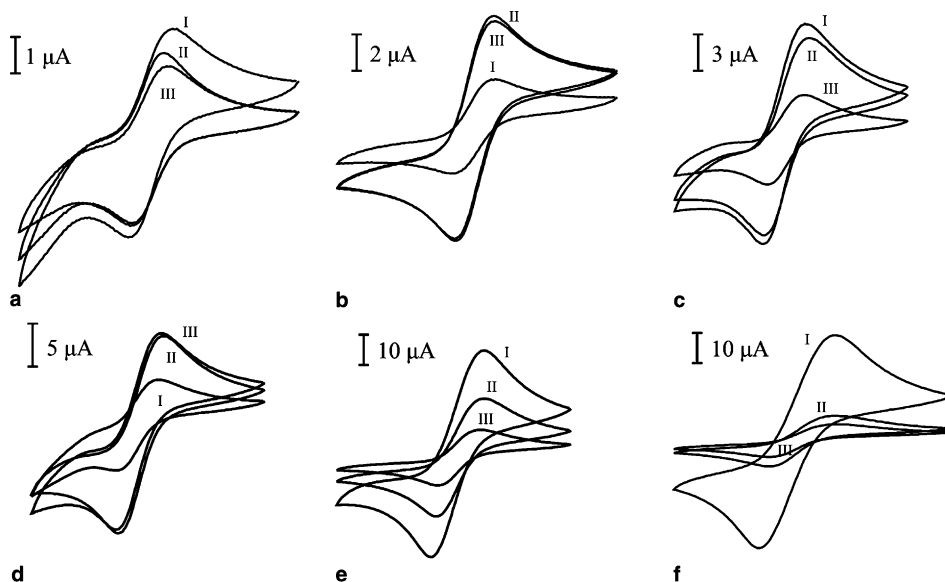


Fig. 6. Stability of PVA-SbQ/VHCF electrodes covered with (a) polycarbonate, (b) polyethyleneimine, and (c) Nafion membranes at 50 mM phosphate, pH 7, buffer solution. The stability of an electrode assembly as (c) in 50 mM Tris buffer solution at pH 7, 8 and 9 is shown in graphs (d), (e) and (f), respectively. Scan rate:  $0.200 \text{ V s}^{-1}$ . (I), 100th scan; (II), 400th scan; (III), 1000th scan.

### 3.4. Electrocatalysis of hydrogen peroxide – analytical performance

As it can be seen from the insets graphs in Fig. 7, no obvious electrocatalysis of  $\text{H}_2\text{O}_2$  was observed when a Nafion/PVA–SbQ (blank) GC electrode was used (inset graph). On the other hand, both anodic and cathodic currents were found to increase at 0.25 and 0.1 V, respectively, indicating that VHCF material electrocatalyzes both the oxidation and reduction of  $\text{H}_2\text{O}_2$ . CVgrams in Fig. 7 indicate the successful electron shuttling between the analyte and the electrode surface through a regenerating mediator. The observed catalytic currents in both the anodic and cathodic regions were directly dependent on the hydrogen peroxide concentration.

Based on the results received regarding the working stability of the proposed electrodes, further experiments were carried out in Tris buffer, pH 7. The analytical characteristics of the VHCF-based sensor are displayed in Table 1. The interference effect of various electroactive compounds was also studied. The low working potential and the outer Nafion membrane resulted to interference free sensors.

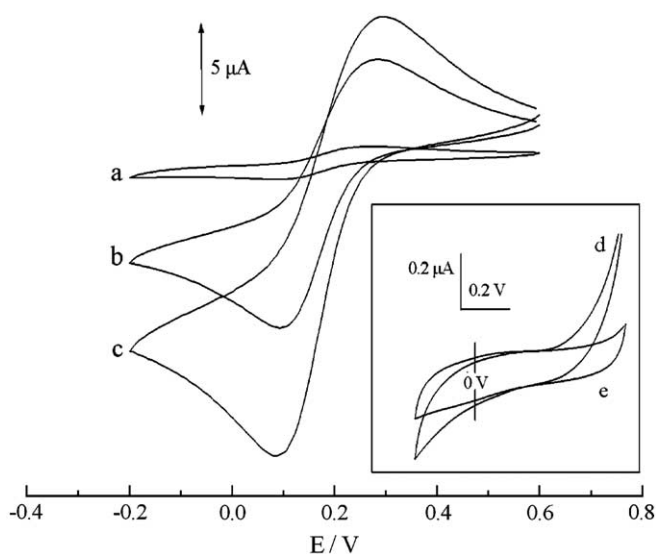


Fig. 7. Cyclic voltammograms illustrating the electrocatalysis of hydrogen peroxide. CV plots of PVA–SbQ/VHCF electrodes at successive additions of hydrogen peroxide (a, 0; b, 2; c, 2 mM). Inset graph: CV plot of a PVA–SbQ covered bare glassy carbon electrode (d) before and (e) after the addition of 12 mM hydrogen peroxide. Scan rate:  $0.100 \text{ V s}^{-1}$ . Buffer solution: 50 mM Tris, pH 7.

Table 1  
Analytical performance of the VHCF-based sensor

Linear range (calibration curve) (mM)	0.01–3.0
$I (\mu\text{A}) = f(C/\text{mM})$	$13.18 C - 0.270$
Correlation coefficient ( $r$ )	0.9996
LOD <sup>a</sup> ( $\mu\text{M}$ )	4
Response time <sup>b</sup> (s)	47

<sup>a</sup> For  $S/N = 3$ .

<sup>b</sup> To retain 90% of the steady state value ( $i_{90}$ ).

Using steady state amperometry, no interference effect was observed even in the presence of 10 mM ascorbic acid.

The working stability of the sensor was verified amperometrically by successive injections of 0.1 mM  $\text{H}_2\text{O}_2$ . As a result, the final activity of the composite films (current response versus initial current response  $\times 100$ ) was almost 85% after 110–120 runs. When not in use, they stored dry at  $+4^\circ\text{C}$  and retained almost 90% of their initial activity after a period of three weeks.

## 4. Conclusions

Vanadium hexacyanoferrate solid with chemical formula,  $\text{K}_2(\text{VO})_3[\text{Fe}(\text{CN})_6]_2$ , was synthesized by mixing  $\text{V}_2\text{O}_5 \cdot n\text{H}_2\text{O}$  xerogel fine powder with ascorbic acid and  $\text{K}_4[\text{Fe}(\text{CN})_6]$  in DDW.

Composite films of PVA–SbQ/VHCF exhibit reversible, almost charge-transfer controlled redox functions and a remarkable electrocatalysis of hydrogen peroxide. The produced transducer offers a low potential detection of  $\text{H}_2\text{O}_2$  at neutral pH and their sensitivity is optimal for various analytical applications.

Nafion protected electrode assemblies found also to be highly selective to hydrogen peroxide, since no response was observed in the presence of 10 mM ascorbic acid.

Stability studies showed that the effect of sodium cations on the redox activity of VHCF films, as it is observed under the specific experimental conditions, can be overcome by employing properly charged coatings.

## References

- [1] M.I. Prodromidis, M.I. Karayannis, *Electroanalysis* 14 (2002) 241.
- [2] L. Gorton, *Electroanalysis* 7 (1995) 23.
- [3] A. Chaubey, B.D. Malhotra, *Biosen. Bioelectron.* 17 (2002) 441.
- [4] Y. Xu, W. Peng, X. Liu, G. Li, *Biosen. Bioelectron.* 20 (2004) 533.
- [5] M. Delvaux, A. Walcarius, S. Demoustier-Champagne, *Anal. Chim. Acta* 525 (2004) 221.
- [6] P. Day, F. Herren, A. Ludi, H.U. Gudel, F. Hulliger, D. Givord, *Helv. Chim. Acta* 63 (1980) 148.
- [7] K. Itaya, T. Ataka, S. Toshima, *J. Am. Chem. Soc.* 104 (1982) 4767.
- [8] A.A. Karyakin, E.E. Karyakina, L. Gorton, *Electrochim. Commun.* 1 (1999) 78.
- [9] A. Ludi, H.U. Gudel, *Struct. Bond.* 14 (1973) 1.
- [10] K. Itaya, I. Uchida, V.D. Neff, *Acc. Chem. Res.* 19 (1986) 162.
- [11] J.J. Garcia-Jareno, A. Sanmatias, J. Navarro-Laboulais, F. Vicente, *Electrochim. Acta* 44 (1998) 395.
- [12] F. Ricci, G. Palleschi, *Biosen. Bioelectron.* 21 (2005) 389.
- [13] P.A. Fiorito, S.I. Cordoba de Torresi, *J. Electroanal. Chem.* 581 (2005) 31.
- [14] W. Tao, D. Pan, Y. Liu, L. Nie, S. Yao, *Anal. Biochem.* 338 (2005) 332.
- [15] D. Ivekovic, S. Milardovic, B.S. Grabaric, *Biosens. Bioelectron.* 20 (2004) 872.
- [16] X. Cui, L. Hong, X. Lin, *J. Electroanal. Chem.* 526 (2002) 115.
- [17] A.A. Karyakin, *Electroanalysis* 13 (2001) 813.
- [18] A. Eftekhari, *Talanta* 55 (2001) 395.
- [19] I. Luiz de Mattos, L. Gorton, T. Laurell, A. Malinauskas, A.A. Karyakin, *Talanta* 52 (2000) 791.
- [20] J. Wang, X. Zhang, M. Prakash, *Anal. Chim. Acta* 395 (1999) 11.
- [21] R. Garjonyte, A. Malinauskas, *Sens. Actuat. B* 56 (1999) 93.

- [22] M.S. Lin, W.C. Shin, *Anal. Chim. Acta* 381 (1999) 183.
- [23] Y. Mishima, J. Motonaka, K. Maruyama, S. Ikeda, *Anal. Chim. Acta* 358 (1998) 291.
- [24] S.A. Jaffari, A.P.F. Turner, *Biosens. Bioelectron.* 12 (1997) 1.
- [25] M. Florescu, C.M.A. Brett, *Anal. Lett.* 37 (2004) 871.
- [26] W.S. Cardoso, M.S.P. Francisco, A.M.S. Lucho, Y. Gushikem, *Solid State Ionics* 167 (2004) 165.
- [27] R. Pauliukaite, M. Florescu, C.M.A. Brett, *J. Solid State Electrochem.* 9 (2005) 354.
- [28] D. Shaojun, L. Fengbin, *J. Electroanal. Chem.* 210 (1986) 31.
- [29] M.K. Carpenter, R.S. Conell, S.J. Simko, *Inorg. Chem.* 29 (1990) 845.
- [30] Y. Wang, G. Zhu, E. Wang, *J. Electroanal. Chem.* 430 (1997) 127.
- [31] C.W. Liu, S.J. Dong, *Electroanalysis* 9 (1997) 838.
- [32] K.K. Kasem, *J. Appl. Electrochem.* 31 (2001) 1125.
- [33] P.N. Trikalitis, V. Petkov, M.G. Kanatzidis, *Chem. Mater.* 15 (2003) 3337.
- [34] P.H. Zhou, D.S. Xue, H.Q. Luo, J.L. Yao, H.G. Shi, *Nanotechnology* 15 (2004) 27.
- [35] N.R. de Tacconi, K. Rajeshwar, R.O. Lezna, *Chem. Mater.* 15 (2003) 3046.
- [36] F.A. Miller, C.H. Wilkins, *Anal. Chem.* 24 (1952) 1253.
- [37] C.G. Tsiafoulis, A.B. Florou, P.N. Trikalitis, T. Bakas, M.I. Prodromidis, *Electrochem. Commun.* 7 (2005) 781.
- [38] D. Shaojun, L. Fengbin, *J. Electroanal. Chem.* 217 (1987) 49.
- [39] J.J. Garcia-Jareno, J. Navardo-Laboulais, F. Vicente, *Electrochim. Acta* 41 (1996) 2675.